Journal of Engineering Technology and Applied Physics

An Absolute Phase Estimation Method for Interferometry Imagery

Sui Ping Lee*, Yee Kit Chan and Tien Sze Lim
Faculty of Engineering and Technology, Multimedia University, Jalan Ayer Keroh, 75450, Melaka, Malaysia
*Lee.sui.ping.zte@gmail.com
https://doi.org/10.33093/jetap.2019.1.2.4

***Abstract* - Accurate interpretation of interferometric image requires an extremely challenging task based on actual phase reconstruction for incomplete noise observation. In spite of the establishment of comprehensive solutions, until now, a guaranteed means of solution method is yet to exist. The initially observed interferometric image is formed by 2π-periodic phase image that wrapped within (-π, π]. Such inverse problem is further corrupted by noise distortion and leads to the degradation of interferometric image. In order to overcome this, an effective algorithm that enables noise suppression and absolute phase reconstruction of interferometric phase image is proposed. The proposed method incorporates an improved order statistical filter that is able to adjust or vary on its filtering rate by adapting to phase noise level of relevant interferometric image. Performance of proposed method is evaluated and compared with other existing phase estimation algorithms. The comparison is based on a series of computer simulated and real interferometric data images. The experiment results illustrate the effectiveness and competency of the proposed method.**

Keywords—Interferometric filter, phase unwrapping, interferometry phase estimation, phase noise suppression

I. INTRODUCTION

Over the past decades, there has been a marked increase in the importance of absolute phase estimation for interferometric imaging techniques [1-3]. Estimation of absolute phase (also known as phase unwrapping) plays as the core technology for many classes of renowned interferometry imagery cover interferometry synthetic aperture radar InSAR, magnetic resonance imaging MRI and etc. During InSAR imagery, the phase difference image (also known as interferogram) is extracted based on coherent field backscattered from illuminated surface using two SAR sensors that separated by baseline. Phase unwrapping plays as the key role to reconstruct the observed interferogram into the meaningful phase value for its geophysical application [4]. For MRI system, phase unwrapping also appears as essential processing step to solve the problem of water/fat separation and noise distortion issue from the observed phase image [5]. Additionally, the optical interferometer imaging also requires technique of absolute phase estimation for accurate image interpretation [6]. Thus, this research topic has risen as a highly concern problem for several prestigious research communities.

Aforementioned interferometric applications related the observed phase value with the absolute phase value in a non-linear and noisy condition. Such nonlinearity is due to noise induced during the radio wave propagation mechanism of sinusoidal acquisition. Therefore, the sinusoidal system forms a noisy 2π-periodic phase image that wrapped within (-π, π]. This is an ambiguous observation since the meaningful phase value of InSAR observation should be the 'unwrapped' absolute phase that located outside (-π, π] and that could be hundreds or thousands radian. The task to reconstruct such wrapped value to its absolute phase value is known as phase unwrapping. In interferometry field, phase unwrapping also well-known as the most difficult task since the necessary phase information is not available for reconstruction of actual phase [7]. Despite of enormous research efforts, the determination of absolute phase for interferometric image still remain open.

Recovery of actual phase from such inverse problem is improbable, but absolute phase estimation based on assumption is still possible. This paper assumes the existence of single dominant back scatterer in each resolution element over observed interferometric image [8] and scope down the absolute phase estimation task as a relatively inferring task of phase value based on adjacent sample pixels in which the determination of the constant or offset phase value is not considered as part of phase unwrapping (or absolute phase estimation).

Section II explains the signal model and the problem statement while the working mechanism of proposed method is described in section III. Incorporated aforementioned de-noising framework, this paper introduces an algorithm solver for interferometric phase estimation. Similar to other

Published by MMU PRESS. URL: https://journals.mmupress.com/index.php/jetap/index

interferometric phase estimation methods, our proposed method incorporates the preliminary processing step of Itoh's phase unwrapping to estimate on the absolute phase value for interferometric image [9]. Different than conventional Itoh's phase unwrapping, the anticipated Itoh's method working in such a way that following guidance of an improved order statistical filters. By adapting to phase noise level of interferometric observation, the improved order statistical filter capable to perform noise suppression with appropriate information preservation. In Section IV, proposed algorithm is validated through a series of computer simulated data and real interferometric data set based on InSAR imagery in which a performance evaluation is included to assess the competency of proposed algorithm as compared to other existing interferometric phase estimation method.

II. Interferometric Signal Model and its Problem Formulation

The working nature of interferometry system is based radio echo of sinusoidal wave [10] in which the measured signal could be represented by a complex-valued signal model as $S_{observed}$. In InSAR system, the observed data of $S_{observed}$ is extracted from two SAR observed complex-valued images of S_1 and S_2 based on n number of look as $s_{observed} = \frac{1}{n}\sum S_1(.)S_2^*(.)$. $S_2^*(.)$ refers to conjugate value of S_2. As mentioned before, the observed signal might consist of noise distortion. Thus, the two-dimensional noisy measurement of $S_{observed}$ is modelled as (1) in which $n(.)$ stands for the random variables that indicates on the complex noise. The imaginary number is indicated by j. $S_T(.)$ denotes the signal model that represents actual value for interferometry application. For polar form equations, $S_T(.) = e^{j\psi_T}$ and $n(.) = e^{j\psi_n}$.

$$s_{observed}(x,y) = s_T(x,y)n(x,y) = e^{j\psi_T}e^{j\psi_n} \quad (1)$$

For interferometry imagery, we are concerning on observed phase images Ψ_{ob} that could be extracted from complex-value interferometric data $S_{observed}$ whereby $S_{observed}(.) = e^{j\psi_{ob}}$.The interferometric phase statistics have been extensively studied in many contexts [3, 7, 9] and the phase noise is characterized by Lee *et al.* [11, 12] based on an additive statistics as Eq. (2) in which Ψ_{ob} denotes observed phase value while Ψ_T indicates the actual interferometric phase for actual measurement. Ψ_n stands for the phasor noise.

$$\psi_{ob} = \psi_T + \psi_n \quad (2)$$

As mentioned in previous section, Ψ_T is a larger value that lay outside (-π, π] with multiple jump count number k of 2π. However, the working mechanism interferometry extracted only wrapped observation value Ψ_{ob} that wrapped by $W(.)$= *modulus* (-π, π]. Equation (3) describes such circumstance.

$$\psi_{ob} = W(\psi_T) \in \{-\pi, \pi]$$
$$\psi_T = \psi_{0b} + 2\pi k \quad (3)$$

This paper incorporates the one-look interferometric phase distribution ($m = 1$) that derived by Lee *et al.* [11] based on the correlation level of relevant interferometric image as shown in Eq. (4).

$$P_n(\psi_n) = \frac{\Gamma\left(m+\frac{1}{2}\right)(1-|\gamma|^2)^m\beta}{2\sqrt{\pi}\Gamma(m)(1-\beta)^{\frac{m+1}{2}}} + \frac{(1-|\gamma|^2)^m}{2\pi} \cdot F\left(m, 1; \frac{1}{2}; \beta^2\right)$$
$$, -\pi < (\psi_n - \theta_c) \leq \pi \quad (4)$$

F(.) refers to Gauss hyper geometric function $\beta = |c|cos(\psi_n - \theta_c)$. Γ is gamma function while m refers to number of look with m = 1 based on single look complex images. θ_c refers to the phase of complex correlation coefficient γ which can be computed as Eq. (5). The formulation of γ is shown as below when E[.] stands for the expected value.

$$\gamma = \frac{E[S_1 S_2^*]}{\sqrt{E[S_1]^2 E[S_2]^2}} = |\gamma|e^{j\theta_c} \quad (5)$$

Figure 1 shows the plotting of interferometric phase distribution based on different level of correlation level based on Eq. (4); from which, the shape of relevant distribution seem to be more concentrate on the center value of zero mean with the rise of correlation level. This plotting seems to be show that the value of standard deviation might reduce due to the increment of correlation level. Figure 2 plots the standard deviation of interferometric phase versus correlation. Hence, these finding provides more evidences for the aforementioned relationship of interferometric error and correlation.

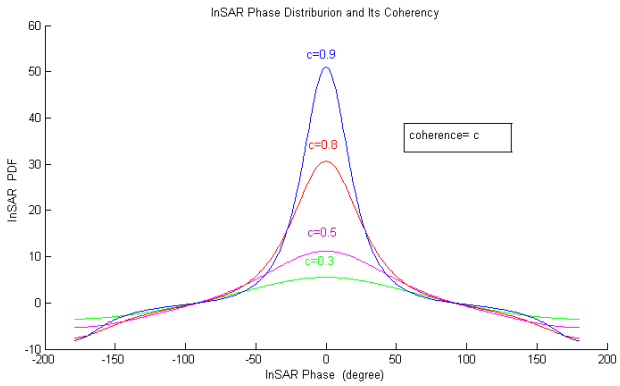

Fig. 1. Interferometric phase distribution based on different level of correlation.

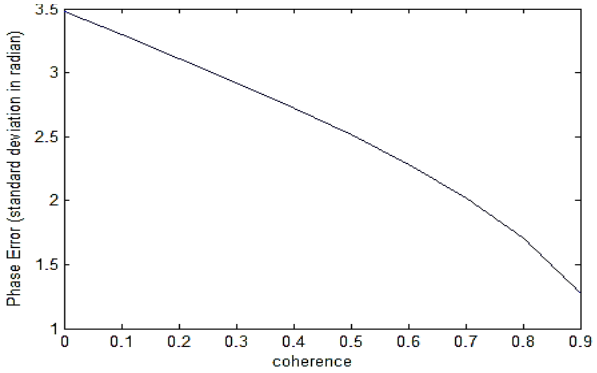

Fig. 2. Interferometric phase error based on different level of correlation.

III. Proposed Absolute Phase Estimation Method

The proposed phase estimation methods for two dimensional 2D interferometric imaging covers phase noise suppression, blindly phase discontinuities preservation and phase unwrapping. As shown in Fig. 3, the working principals of proposed method are described by following processing steps.

A. Step 1: Extraction of Interferometric Phase Image

The interferometry processing requires the two dimensional observation of phase arrays that could be extracted from the complex-valued input signal of the radio echo waves. For InSAR processing, formation of interferogram Ψ_{ob} involves of the extraction of phase difference image $\Delta\Theta$ among the input SAR images of S_1 and S_2 from different aperture views to same target of illuminated area. Equation (6) describes the computation task to extract on interferometric wrapped phase based on InSAR system.

$$\psi_{ob} = \Delta\Theta = \vartheta_1 - \vartheta_2 = arg[S_1 S_2^*] = arg\left(|S_1||S_2|e^{i(\vartheta_1-\vartheta_2)} \in (-\pi,\pi]\right) \quad (6)$$

B. Step 2: Estimation of Coherence Level

Analytical study of section II shows decrement of interferometric phase error with increment of coherence level. In many contexts of InSAR experiments [13, 14], the coherence values are used as the 'measured' of noise. Thus, the proposed method incorporates a coherence map to 'assess' on the noise level of its observed interferometric images. In practice, the coherence level of relevant interferometric phase image can be estimated by computing on correlation level among the pair (or pairs) of its complex-valued observations where $Co[.]$ refers to the coherence map while $\overline{s_1} = E[{S_1}^2]$ and $\overline{s_2} = E[{S_2}^2]$. Co is used as the important indicator or parameter estimator of an order statistical filter for the task of phase estimation.

$$Co[.] = \frac{E[S_1 S_2^*]}{\sqrt{\overline{s_1} \times \overline{s_2}}} \in [0,1] \quad (7)$$

C. Step 3: Improved Order-statistical Filter

The proposed algorithm incorporates a non-linear spatial filter base on the coherence weighted order-statistical filter for noise suppression. Unlike other order-statistical filter with fixed size window, the improved order statistical filter able to adjust the size of its filtering window for different level of noise by referring to the coherence map that generated by previous step. By refer to the plotting of interferometric phase standard deviation as Fig. 2. The proposed method intends to preserve the pixel with potential phase discontinuity by setting the coherency level of 0.3 as the threshold parameter in which all phase information with Co < 0.4 is blindly preserved while the pixel with larger value of Co is go through on the minimum order statistical filter for image restoration based on the first-order neighbor pixels. Such working step enables the preservation of information and prevent on the problem of over-filtering during the task of noise suppression. Equation 8 describes the improved order statistical filter F(.) where $\{\varphi(x-1,y), \varphi(x+1,y), \varphi(x,y+1), \varphi(x,y-1)\}$ refers to the first order neighbor of target pixel respect to target filter pixel of $\varphi(x,y)$.

$$F(\varphi(x,y)) = \min_{(x,y)\in w_I} \{\varphi(x,y)\}, \text{ where}$$

$$w_I = \begin{cases} \{\varphi(x,y)\} & , \text{Co} > 0.4 \\ \{\varphi(x-1,y), \varphi(x+1,y), \varphi(x,y+1), \varphi(x,y-1)\} & , Co \le 0.4 \end{cases} \quad (8)$$

D. Step 4: Two Dimesional Phase Unwrapping

Previous step performed the noise suppression task and preserved the phase information of the highly corrupted pixel in which the processing outcome of step 3 is the wrapped phase image after noise reduction $\phi(.)$. In this step, two dimensional phase unwrapping is performed in order to infer on the absolute phase value from the wrapped phase ϕ. Eq. (9) describe the working mechanism of 2D phase unwrapping where $\hat{\varphi}$ denotes the estimated phase value while ϕ denotes the processing outcome of step 3. The jump count of k could be estimated based on column adjustment k_{col} and row adjustment k_{row}. The phase gradient Δ is computed by the value different along two adjacent pixels. $\Delta column$ indicates on the horizontal phase gradient while Δrow refers to the vertical phase gradient of interferometric image.

$$\hat{\varphi}(x,y) = \emptyset(x,y) + 2\pi\left[\sum_{x=1}^{m} k_{column}(x,y) + \sum_{y=1}^{n} k_{row}(x,y)\right],$$

given that

$$k_{col}(x,y) = \begin{cases} 0 & , \Delta column \le \pi \\ 1 & , \Delta column \ge \pi \cap [\emptyset(x-1,y) > \emptyset(x,y)] \\ -1, & \Delta column \ge \pi \cap [\emptyset(x-1,y) < \emptyset(x,y)] \end{cases}$$

$$k_{row}(i,j) = \begin{cases} 0 & , \Delta row \le \pi \\ 1 & , \Delta row \ge \pi \cap [\emptyset(x.y-1) > \emptyset(x,y)] \\ -1, & \Delta row \ge \pi \cap [\emptyset(x,y-1) < \emptyset(x,y)] \end{cases} \quad (9)$$

E. Step 5: Smoothing Filter

Recalled that the step 4 has blindly preserved the data pixel of high coherency zone in which the noise suppression is not being performed on relevant zone. After the 2D phase unwrapping, the over-filtering is less likely to be happened. Therefore, the extensive noise filtering task could be performed in this step. The step 5 incorporates an averaging filter with 4 × 4 window size as smoothing filter. The averaging filter is repeated for l times until the outcome image become the satisfied image between based on visual assessment. The final processing outcome of step 5 produces the estimated outcome of the proposed method.

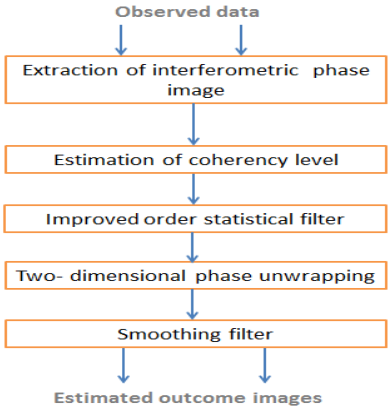

Fig. 3. Working procedures of proposed method.

IV. Performance Tests

In order to evaluate on the performance of proposed method, this section performs several experimental tests based on three series of interferometric data covers the simulated noisy scene, extreme scene and real InSAR scene of Long

Peak mountainous. For comparative studies, the performance tests also cover several mandatory interferometric phase unwrapping methods which are Goldstein Branch cut method, Phase unwrapping via graph cut (also known as PUMA method) and Quality map guided method. Such experiment tests are implemented based on the computer with specification of Intel(R) Core(TM) i5-3210M CPU @ 2.50 GHz, 2501 MHz, 2 Core(s) and 4 Logical Processor(s).

A. Experiments of Noisy Interferometric Observations

This section performs the experimental tests based on the simulated test scene of noisy interferometry observations with 17 dB signal-to-noise ratio as shown in Fig. 4. Figure 4(a) represent the two dimensional image of actual phase while Fig. 4(c) shows the 3D surface structure of relevant terrain. Fig. 4(b) refers to the measured phase images of interferogram while Fig. 4(d) presents the estimated outcome of proposed method. For comparative study, Fig. 5(e) shows unwrapped phase image of Goldstein branch cut method and Fig. 4(f) indicates unwrapped phase image of PUMA method. Figure 4(g) refers to unwrapped phase image of quality map guided method. From the visual assessment, all tested algorithms have well-reconstructed on the surface structure for the noisy interferometric observation in which the shape of surface structure are accurately reshaped as compare to Fig. 4(a) of actual phase image.

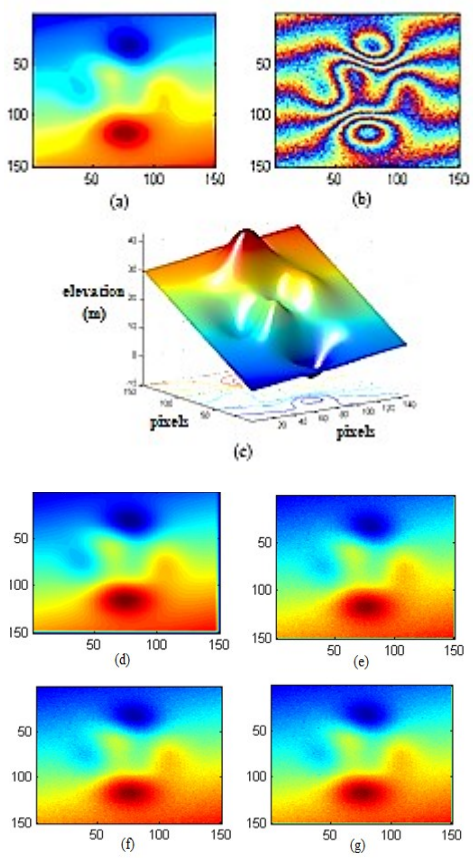

Fig. 4. Experimental results: (a) actual phase image, (b) observed noisy interferogram, (c) 3D surface structure plot of actual phase, (d) estimated phase of proposed method, (e) unwrapped phase of Goldstein branch-cut method, (f) unwrapped phase of PUMA method and (g) unwrapped phase of quality map guided method.

B. Extreme Scene: Noise, Aliasing and Exreme Surface Structure

In this section, the experiments target to exanimate the interferometric phase estimation methods based on the computer generated scenes that induced by multiple problems covers noise, aliasing and extreme surface. The simulation scenes are based on InSAR applications where the assumptions of non-aliasing condition are violated. This simulation imitates the challenging non-linear circumstance of real InSAR observations. Figure 5(a) shows the image of actual phase and Fig. 5(c) generates the 3D surface structure of relevant sharply peak. Figure 5(b) shows the measured phase images of noisy interferogram which is the observation image. Figure 5(d) shows the estimated outcome of proposed method. Figure 5(e) presents unwrapped phase image of Goldstein branch cut method and Fig. 5(f) indicates unwrapped phase image of PUMA method. Figure 5(g) refers to unwrapped phase image of quality map guided method.

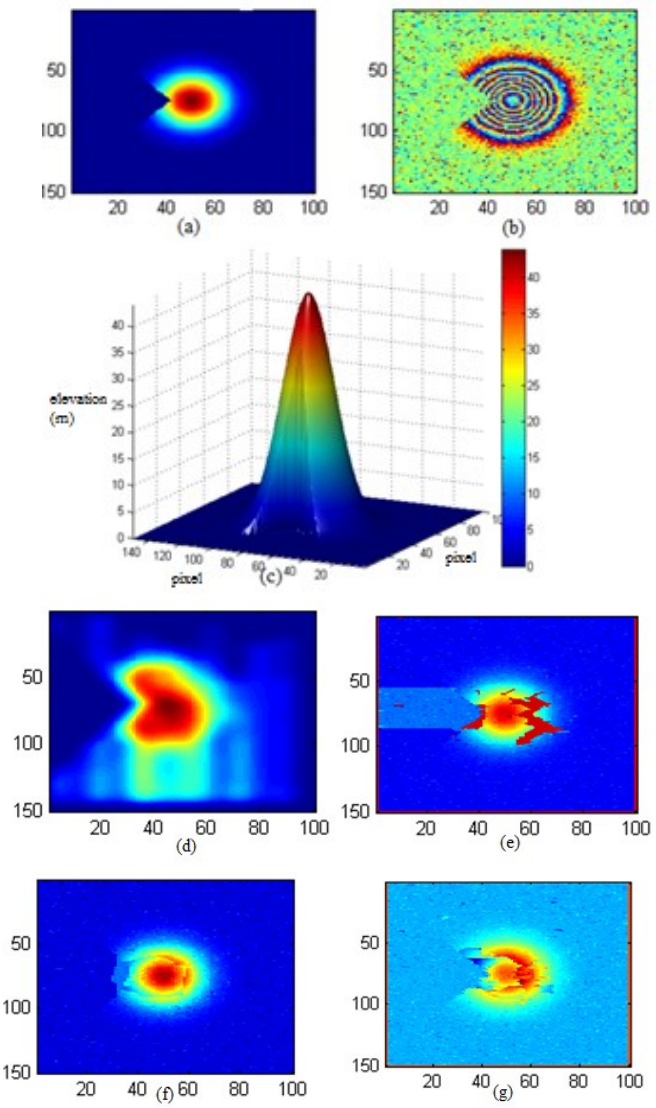

Fig. 5. Experimental results of extreme scene tests: (a) actual phase image, (b) observed noisy interferogram, (c) 3D plot of terrain surface based on actual phase value, (d) estimated phase image of proposed method, (e) unwrapped phase image of Goldstein branch cut method, (f) unwrapped phase image of PUMA method and (g) unwrapped phase image of quality map guided method.

Since the conditions of extreme scenes have violated most of the assumptions of all interferometric phase estimation methods, all of the estimated results contain flaws. From the visual assessment from Fig. 5, the outcome results of Goldstein branch cut Fig. 5(e) consists high error over central area of mountain region; this is because branch-cut method has leaved 'null' solution over the aliasing zone. In Fig. 5(f), it can be observed that the PUMA method is well-resist to aliasing problem by well-construct on relevant surface area. However, PUMA has failed to detect the extreme surface in which the notch area is wrongly reshaped as part of a complete round-shaped hill. In Fig. 5(g), the unwrapped phase image of quality map guided method partly degraded by aliasing and notch surface. Compare to other methods, proposed method show good resistance at both aliasing and extreme surface problem; however, the bottom part of estimated images consists of little errors that accumulated from aliasing or extreme surface zone.

C. Real Scene: InSAR Observation of Long Peak Mountainous

In this section, the experiments incorporate the real interferometric data scenes that generated from John Hopkins University based on InSAR measurement over Long Peak, Colorado, United States [9]. The actual ground truth data is also provided in relevant data set. Figure 6 shows relevant data set and estimation results of aforementioned interferometric phase estimation method which cover (a) actual phase image, (b) observed noisy interferogram, (c) 3D plot of terrain surface based on actual phase value, (d) estimated phase image of proposed method, (e) unwrapped phase image of Goldstein branch cut method, (f) unwrapped phase image of PUMA method and (g) unwrapped phase image of quality map guided method. In overall, the visual assessment shows that almost all methods are success to construct on the surface structures of Long Peak mountainous unless the unwrapped phase image of Goldstein branch cut method (as shown in Fig. 6(e)) shows some obvious "null" error over cliff regions (upper part).

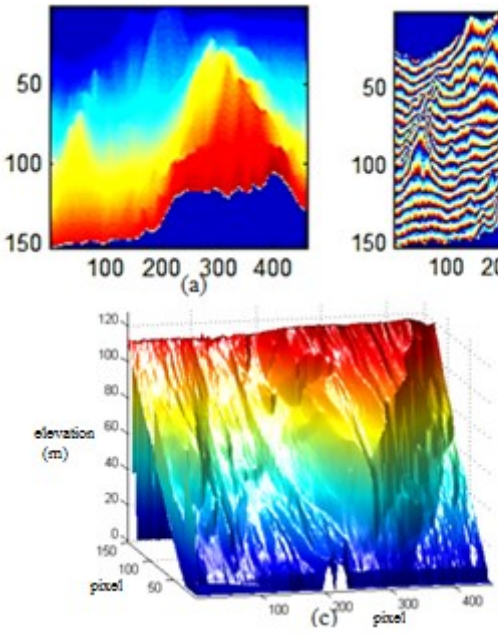

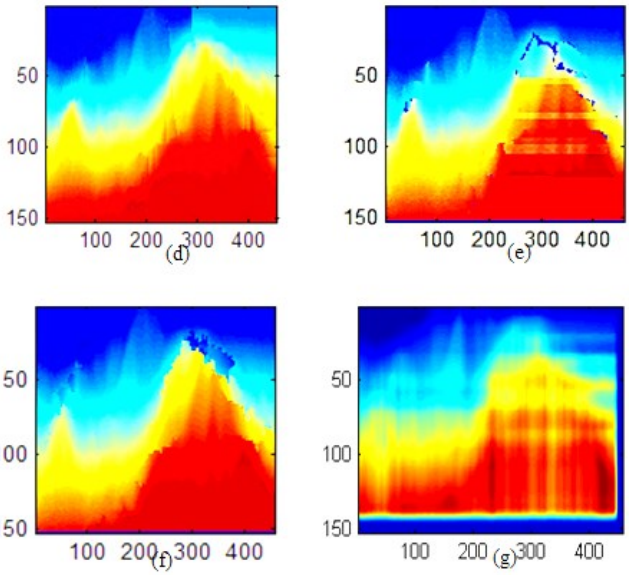

Fig. 6. Experimental results of Long Peak Mountainous scene : (a) actual phase image, (b) observed noisy interferogram, (c) 3D plot of terrain surface based on actual phase value, (d) estimated phase image of proposed method, (e) unwrapped phase image of Goldstein branch cut method, (f) unwrapped phase image of PUMA method and (g) unwrapped phase image of quality map guided method.

D. Performance Evaluations

Table I. Performance of interfeometric phase estimation methods based on root mean square error.

Interferometric Phase Estimation Methods	**RMSE results for various phase image (in radian)**		
	Noise-induced scene	Extreme scene	Real mountainous scene
Proposed Method	0.0801	0.2230	0.4550
Goldstein Branch-cut Method	1.5395	4.1913	0.5490
PUMA Method	0.5135	0.6166	0.8811
Quality Map guided Method	1.5396	2.5276	0.6075

Table II. Computation times of interfeometric phase estimation methods.

Interferometric Phase Estimation Methods	**Computation time of various size for phase image (in second)**			
	50×50	100×100	200×200	400×400
Proposed Method	0.24	0.30	0.31	0.76
Goldstein Branch-Cut Method	0.57	2.01	7.49	35.91
PUMA Method	0.68	0.73	5.25	47.95
Quality Map guided Method	6.20	11.98	69.62	1292.58

Previous sections show the visualized experiment results for various test scenes in term of images. Other than visual assessment, the accuracy of each method could be also measured by other metric i.e. root mean square error, RMSE. Table I shows the accuracy level for aforementioned phase estimation methods based on each case of test scene using metric of RMSE; from which, the proposed method is up-performed other methods. PUMA method ranked second and

following by Quality Map guided method. Since the working mechanism of branch-cut method leave "null" solution on the certain isolation zone due to residues link, such method produces most inconsistences as compare to other methods [10].

The performance evaluation also includes a complexity test that count on the computation times for the absolute phase estimation methods for various sizes of $N \times N$ interferometric phase images with N = 50, 100, 200, 400. From the results of complexity test in Table II, the proposed method gives fastest processing time, following by PUMA algorithm. Goldstein branch-cut method ranks third in term of time efficiency. Compare to others, the quality map guided method incorporated of an extra phase variance map that has increase on the computation cost of entire algorithm. Therefore, it requires most processing time than others.

V. CONCLUSION

The analytical study of phase ambiguity shows that the interferometric phase error is decreasing corresponding to the correlation level of interferometric input images. Proposed solution performs the phase estimation by incorporated the classical Itoh phase unwrapping procedure that guided by an improved ordered statistical filter. The proposed algorithm has incorporated an improved ordered statistical filter able to adapt to the phase noise level and adjust on its filtering rate for different level of noise based on a coherency map. This method capable to filters off the unwanted noise and preserves the important information without over-filtering problem. The comparative studies shows that the proposed solution up-perform other existing interferometric phase estimation methods.

REFERENCES

[1] A. R. Thompson, J. M. Moran and G. W. Swenson, " Introductory Theory of Interferometry and Synthesis Imaging," *Astronomy and Astrophysics Library*, pp. 59-88, 2017.

[2] S. Lian and H. Kudo, "Phase Unwrapping with Differential Phase Image," *Medical Imaging 2017: Physics of Medical Imaging*, doi:10.1117/12.2255727, 2017.

[3] H. Hongxing, J. M. Bioucas-Dias and V. Katkovnik, "Interferometric Phase Image Estimation via Sparse Coding in the Complex Domain," *IEEE Trans. Geosci. Remote Sensing*, vol. 53, no.5, pp. 2587-2602, 2015.

[4] M. Shimada, "SAR Interferometry," *Imaging from Spaceborne and Airborne SARs, Calibration, and Applications*, pp. 251-302, 2018.

[5] J. Dong, F. Chen, D. Zhou, T. Liu, Z. Yu and Y. Wang, "Phase Unwrapping with Graph Cuts Optimization and Dual Decomposition Acceleration for 3D High-resolution MRI Data," *Magnetic Resonance in Medicine*, vol. 77, no.3, pp. 1353-1358, 2016.

[6] C. Tian and S. Liu, "Phase Retrieval in Two-shot Phase-shifting Interferometry based on Phase Shift Estimation in A Local Mask," *Optics Express*, vol. 25, no.18, pp. 21673-21683, 2017.

[7] G. Franceschetti and R. Lanari, "Synthetic Aperture Radar Interferometry," *Synthetic Aperture Radar Processing*, doi:10.1201/9780203737484-4, pp.167-223, 2018.

[8] P. A. Rosen, S. Hensley, I. R. Joughin, S. N. Madsen, E. Rodriguez and R. M. Goldstein, "Synthetic Aperture Radar Interferometry," *Proceedings of the IEEE*, vol. 88, no. 2, pp. 333-382, 2000.

[9] D. C. Ghighlia and M. D Pritt, *Two-Dimensional Phase Unwrapping: Theory, Algorithms, and Software*, New York, Wiley-Interscience, 1998.

[10] H. A. Zebker and Y. P. Lu, "Phase Unwrapping Algorithms for Radar Interferometry—Residue-cut, Least-squares and Synthesis Algorithms," *J. Opt. Soc. Amer. A*, vol. 15, no. 3, pp. 586–598, 1998.

[11] J. S. Lee, K. Hoppel, S. Mango and A. Miller, "Intensity and Phase Statistics of Multilook Polarimetric and Interferometric SAR Imagery," *IEEE Trans. Geosci. Remote Sensing*, vol. 32, no. 5, pp. 1017-1028, 1994.

[12] J. S. Lee, K. Papathanassiou, T. Ainsworth, M. Grunes and A. Reigber, "A New Technique for Noise Filtering of SAR Interferometric Phase Images," *IEEE Trans. Geosci. Remote Sensing*, vol. 36, no. 5, pp. 1456-1465, 1998.

[13] H. Zebker and J. Villasenor, "Decorrelation in Interferometric Radar Echoes," *IEEE Trans. Geosci. Remote Sensing*, vol. 30, no. 5, pp. 950-959, 1992.

[14] S. Mukherjee, A. Zimmer, X. Sun, P. Ghuman and I. Cheng, "CNN-based InSAR Coherence Classification," *2018 IEEE Sensors*, doi:10.1109/icsens.2018.8589742, 2018.